Balanced Boomerangs

Manuel Schütz

December 3, 2020

Abstract

"Dabbes" Klaus H. Dabelstein introduced these kinds of boomerangs in 1987. He considered the classical shape with an annulus sector as elbow. The blade lengths are chosen such that the center of mass of the entire boomerang coincides with the annulus sector center. I widen the balanced boomerang shapes by two more possibilities: The omega and the non symmetrical multi bladed boomerang. I consider more realistic semistadium shaped blades instead of rectangular ones. These balanced shapes may be useful for analytic lift- and drag calculations as these boomerang types can all be seen as a combination of a flying ring and blades. The latter helps to understand how boomerangs can be trimmed. Additionally these shapes have a special appearance during the flight.

1 Glossary of terms

- center of pressure: Where the sum of all aerodynamic forces act.
- annulus sector: central angle 2β, middle radius R, inner radius $r_1 = R - r$, outer radius $r_2 = R + r$. Note that for multibladers, R denotes the outer radius of the annulus.
- auxiliary angle: $\gamma = \frac{\alpha}{2}$.
- auxiliary functions of c: p and q.
- blades: N wings or blades are composed of a rectangle (rectangular blade) or rectangle and semicircle. (semistadium shaped blade). For multi bladed boomerangs: blade i points at angle φ_i. The x axis of the coordinate system corresponds to $\varphi = 0$.
- boomerang coordinate system: For boomerangs with two blades the y-axis is a symmetry axis. For multi bladed boomerangs: orientation is arbitrary.
- boomerang elements: each boomerang is decomposed into $i = 1 \ldots n$ non intersecting rectangles, semicircles, small rectangles, annulus sectors with mass m_i, area A_i and c.o.m located at $\vec{r}_i = \overrightarrow{OS}_i = (x_i, y_i)^T$.
- center of mass of entire boomerang c.o.m: Located at the origin of the boomerang coordinate system.
- classical boomerang: v-shaped, composed of two equal blades connected by an annulus sector.
- joint angle of blades (classical or omega boomerang): α.
- number of boomerang elements: n.

- omega boomerang: looks like the capital greek letter Ω, composed of two equal blades and two small rectangles, connected by an annulus sector.
- rectangle: width b, length ℓ.
- scaling parameter $c = \frac{b}{w}$. Determines how "slim" the boomerang shape is.
- semicircle: radius $r = \frac{b}{2}$.
- small rectangle: width $\frac{b}{2}$, length b.
- wing- or blade length: $w = \ell$ (rectangular blades) or $w = \ell + r$ (semistadium shaped blades)

For transposed vectors I use the shortcut ^{T}.
Boxed equations are results, all other equations are part of the derivations.

2 Introduction: The not so neutral elbow of boomerangs

The elbow of a boomerang connects the two lift creating blades. The idea of "Dabbes" published in [1] and [2] was, that the elbow would have no aerodynamic impact. This however is not true even for an elbow without airfoil. A first reason is the slightly tilted rotation axis of the spinning boomerang: The angle between translational speed vector and rotation axis is not 90° [3], [4], [5]. The boomerang rotation disc thus meets the incoming airflow at a certain collective angle of incidence. The elbow contributes to overall lift. Maybe the remark by the editors of the "Bumerangwelt" in the 1995 no.2 edition [9] that ".... (we) believe that we have already dealt with the topic exhaustively" was a bit early?
In part 1 of the theory I show that balanced boomerangs can be seen as the sum of a flying ring (like the famous Aerobie) and two or more wings attached to it. This allows to explain why the elbow can be used for trimming the shape of the flightpath (higher or lower) without changing the flight range. Just the lift distribution is modified but not overall lift. I wonder: Did the aborigines apply this method?
In part 2 I derive the formulae for three different balanced boomerang types: The classical shape (where "Dabbes" never published the equations to my knowledge), the omega shape (vaguely mentioned in [9]) and multi bladed boomerangs. Someone constructed a balanced non symmetrical three bladed boomerang called "Why-not" resp. "Y-not" in the mid 1980's. Despite the lack of evidence that these balanced boomerangs outperform shapes with less symmetries, it may contribute to better understanding of the dynamics of boomerang. Additionally I was wondering how "Dabbes" did the math, what his assumptions were. I provide exact and approximative solutions and if you want to construct classical or omega shapes without any formulae, look up graphs for direct application have been created in section 4.5.

3 Theory, part 1

What makes a boomerang balanced is, that

1. the elbow has a shape of an annulus or an annulus sector and
2. the center of mass c.o.m of the entire boomerang equals the center of the annulus sector (or annulus for multi bladed boomerangs).

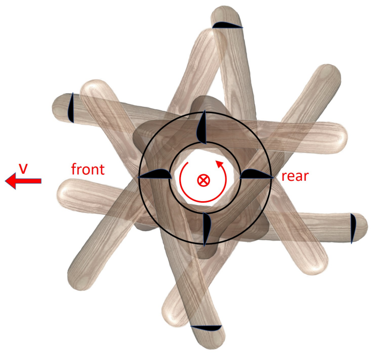

Figure 1: Averaged over one revolution the elbow of a boomerang can be seen as a flying ring like the Aerobie. The elbow can have two local extreme values of lift at the front part and the rear part of the ring. With the pictured airfoil: Maximum at rear, minimum (negative lift) at front. In contrast, the blades produce maximum/minimum lift at halfway between rear and front.

Fig. 3 shows three examples. Now how does the elbow change the flightpath? Even for an arbitrary classical boomerang shape the trace of the elbow during one revolution forms a blurred annulus. See Fig. 1. Note that the boomerang flies from right to left, spinning anti clockwise (right handed throwing for the entire article assumed). Taking a balanced boomerang will trace a sharp annulus when spinning. In contrast to the blades which generate maximum lift halfway between rear and front, [3], [4], the elbow creates maximum lift when being at the rear and minimum lift at the front part of the blurred annulus. Or vice versa, depending on it's airfoil. For a circular arc as airfoil, lift in front/rear part is about equal as such an airfoil creates lift even at zero angle of attack [7]. Michael Siems introduced a neat tool called "Konstruktionsscheibe" (construction disc) [8] which predicts the flightpath as "low" or "high". I translate it into text form: Any lift created behind the c.o.m causes the boomerang rotation axis to nutate according to the left hand rule: Your left thumb represents the velocity and closing your fingers indicate the nutation of the rotation axis. Lift created in front of the c.o.m: right hand rule applies. A boomerang nutating in the latter manner will either stay at the same level. It's lift decreases as it slows down due to drag. But this compensates with lift pointing more and more upwards as the boomerang nutates. Or it gains height if drag is small or if thrown with more velocity. Since the straight blades create a large amount of average lift in front of the c.o.m, overall (blades plus elbow, [3], [4]), the right hand rule applies: Depending on how you design the elbow, the boomerang nutates faster or slower.

Now take a look at Fig. 2 which compares boomerang elbow trimming with trimming of a flying ring [6]. For both the boomerang elbow and a part of a flying ring during one revolution, aerodynamic lift F for a surface element takes two local extreme values (F_1 and F_2). If we modify the elbow with version A, lift F_2 increases due to the now increased angle of attack at the rear part and F_1 decreases at the front part with possible negative values, while halfway between lift doesn't change. Assuming small angles of attack (highly exaggerated in Fig. 2 for visibility) I assume linear lift theory. Thus the magnitude of the overall lift changes just slightly (if at all), other than the lift distribution. Hence the torque on the boomerang respectively flying ring changes. This causes the rotation axis to nutate with the right hand rule faster (case B) or less fast (case A). Result: a higher (B) or lower (A) flightpath. So with an annulus sector as elbow of a balanced boomerangs, the height of the flightpath can be trimmed even strictly without changing the flight range.

A flying ring can be trimmed with exactly the same rationale as the boomerang despite the very different flight paths: Transform the ring to a truncated conical shell as in Fig. 2 and (instead of flying lower) it will swerve less to the right (or even swerve to the left if the center of pressure moves behind the c.o.m).

I wonder if the aboriginees applied this trimming technique? It's very useful as overall lift doesn't change. An accurate non-returning boomerangs for hunting is thrown parallel to the ground with

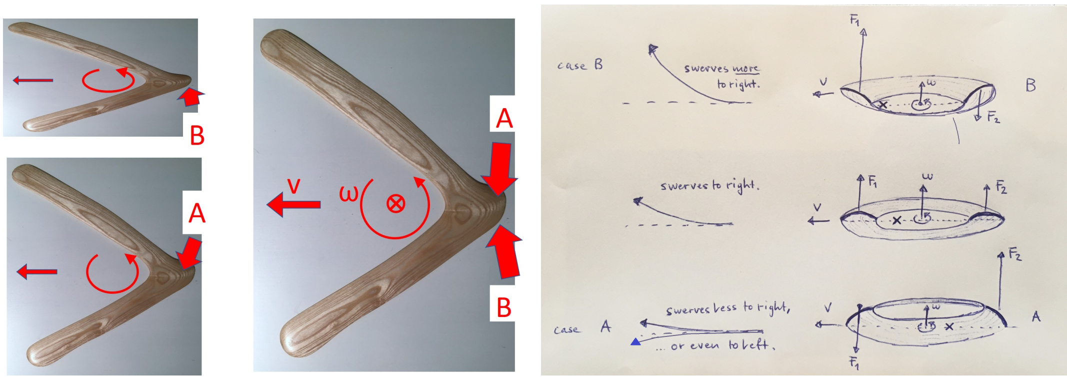

Figure 2: Left: trimming a classical boomerang. Right handed model flying with velocity v, spinning anti-clockwise. Removing material at the outer rim of the elbow from top (A) causes a lower flight as the rotation axis ω nutates more slowly. Removing material from below (B) causes a higher flight due to faster nutation. Note that the averaged lift over one revolution stays the same but the lift distribution changes. This changes the torque hence the change in nutation.
Right: a flying ring can be trimmed in exactly the same way. Version A (trimming exaggerated) will swerve less to the right because the center of pressure $\times$ has moved backwards, decreasing the torque. Or it even swerves to the left. Corresponds to trim version A on the left picture.

rotation axis pointing upwards. It should a) keep it's flight level. Achieved with the right amount of lift and b) fly as straight as possible. The trimming procedure I described fits perfectly as it doesn't change the overall lift.
In [5] and [3] the assumption for the boomerang shape was: equal straight wings pointing away from the c.o.m. They investigated with blade element theory how lift and drag is affected by the speed of the c.o.m, the rotation frequency and the collective angle of incidence (sometimes called "angle of attack"). To investigate more general boomerang shapes, balanced boomerangs could provide quantitative insight about the trimming methods.

4 Theory, part 2

I decompose all boomerang shapes into boomerang elements in order to compute the center of mass per element, then I combine the elements to a boomerang with c.o.m at the origin. A classical boomerang is composed of two rectangles, two semicircles and a matching annulus sector as elbow. An omega consists of an annulus sector, two rectangles, two small rectangles and two semicircles. See Fig 3.
Since the c.o.m. is placed at the origin, the relation

$$\sum_{i=1}^{n} m_i \vec{r}_i = 0 \tag{1}$$

must hold for any boomerang type. The vectors $\vec{r}_i = (x_i, y_i)^T$ point from the origin to the c.o.m of boomerang element i. I assume that the thickness of our boomerang is constant thus c.o.m and

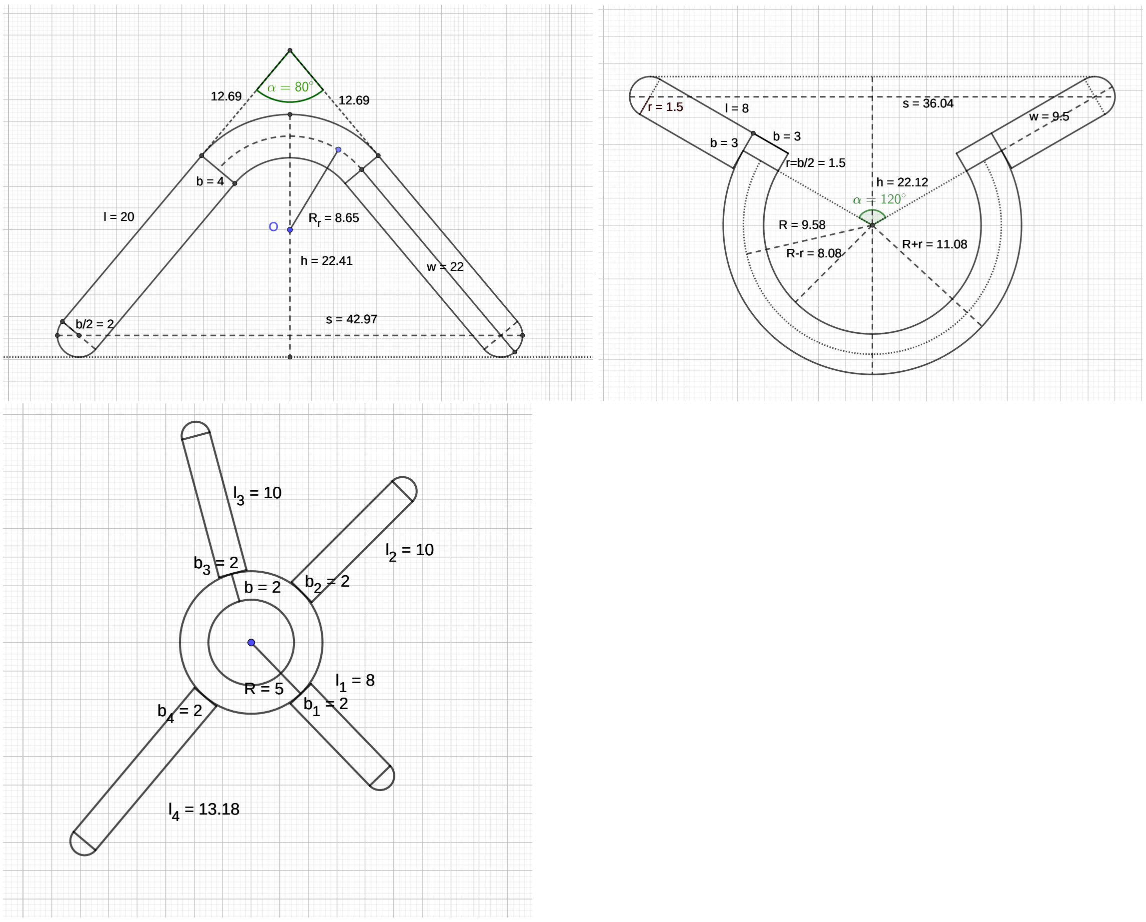

Figure 3: Three types of balanced boomerangs: classical-, omega- and multi bladed boomerang. In all cases the center of mass equals the center of the annulus sector.

center of area are equivalent. I replace m_i of each elementary shape with it's area A_i.

$$\sum_{i=1}^{n} A_i \vec{r}_i = 0 \tag{2}$$

4.1 Some center of masses

For a rectangle with it's left lower corner at the origin, width b and length ℓ, the result is obvious:

$$\vec{r}_i = \frac{1}{2}(b, \ell)^T \text{ or } S_i = \left(\frac{b}{2}, \frac{\ell}{2}\right) \tag{3}$$

For an annulus sector centred at $(0,0)$, see Fig. 4, the symmetry axis shall be the positive y-axis and the central angle is 2β. I calculate the center of mass using the surface element $\eta d\eta d\varphi$ instead of the mass element dm .

$$\vec{r}_i = \frac{\int_{r_1}^{r_2} \eta d\eta \int_{-\beta}^{\beta} d\varphi \eta \left(\sin\varphi, \cos\varphi\right)^T}{\int_{r_1}^{r_2} \eta d\eta \int_{-\beta}^{\beta} d\varphi} = \frac{2\sin\beta\left(r_2^3 - r_1^3\right)}{3\beta\left(r_2^2 - r_1^2\right)}(0,1)^T \tag{4}$$

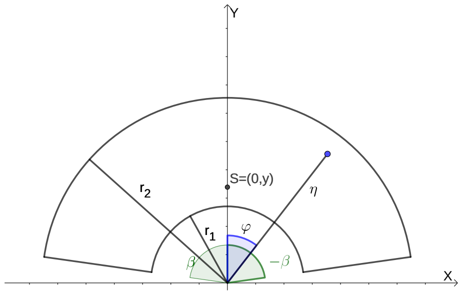

Figure 4: Center of mass of an annulus sector. Includes the special case semicircle if $r_1 = 0$ and $2\beta = \pi$. The integration variables are η and φ.

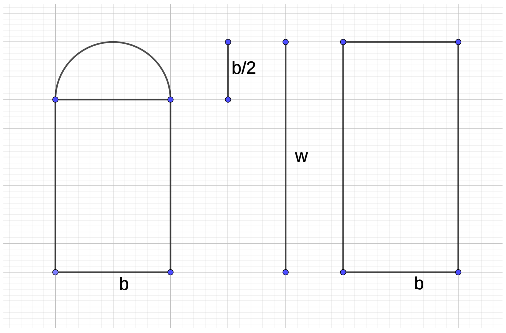

Figure 5: Shape of the boomerang wings and limit of the scale parameter $c \geq 0$. Left hand side: semistadium shaped blade. In this case $w \geq \frac{b}{2}$ hence $c = \frac{b}{w} \leq 2$. Right hand side: rectangular blade. Here just $c \geq 0$ applies.

So $x_i = 0$ and for

$$\text{an annulus sector with} \quad r_2 = R + r, r_1 = R - r: \quad y_i = \frac{\left(3R^2 + r^2\right)\sin\beta}{3R\beta} \tag{5}$$

$$\text{a semicircle with} \quad r_2 = r, r_1 = 0, \beta = \tfrac{\pi}{2}: \quad y_i = \frac{4r}{3\pi} \tag{6}$$

All boomerangs have at least two rectangle elements. Since changing b would scale all other parameters like R, ℓ and w, I define the scaling parameter

$$c = \frac{b}{w} \tag{7}$$

If $c = 0$ the wing is a straight line of length w for both wing types. For a semistadium shaped blade in the case of $w = \frac{b}{2}$ the wing is formed by just the semicircle. Hence $0 \leq c \leq 2$ for the latter, see Fig. 5. In my results I express R rather as ratio

$$\frac{R}{w} \tag{8}$$

This simplifies the graphs to lookup R for different angles α at given w and b. See Fig. 7,8,9 and 10. Equations 3-6 are applied to write conditions for the c.o.m. with Eq. 2 in all following cases.

4.2 Boomerangs with rectangular blades

I start with what seems to be the more simple case.

4.2.1 Classical boomerang

Based on the sketch in [2] I assume that "Dabbes" used this model in both contributions in [1] and [2]. The parts to consider, as described in Eq. 6, are:

1. an annulus sector with area

$$A_1 = \frac{2\beta}{2\pi}\pi\left[(R + r)^2 - (R - r)^2\right] = 2\beta R b$$

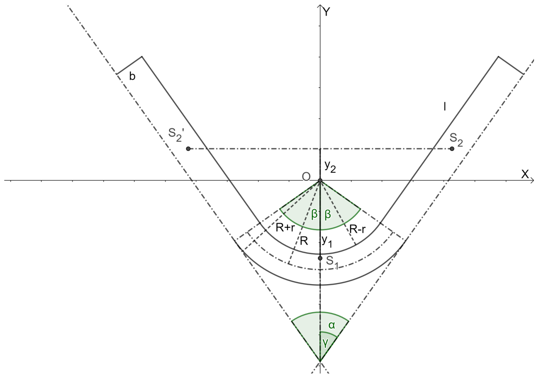

Figure 6: Sketch of the simple "Dabbes definition" classical boomerang. S_1 resp. S_1' are the c.o.m of the rectangular blades. Due to symmetry, only the y-values y_1 and y_2 matter for the c.o.m of the boomerang.

and c.o.m at

$$y_1 = -\frac{\sin\beta}{\beta}\left(R + \frac{b^2}{12R}\right).$$

Recall that $r = \frac{b}{2}$.

2. two rectangles, area

$$A_2 = b\ell$$

each, c.o.m. at

$$y_2 = -R\sin\gamma + \frac{\ell}{2}\cos\gamma.$$

Due to the symmetry the x-components in Eq. 2 can be ignored. However note that $2A_2$ must be inserted as there is a pair of two mirrored parts. See Fig. 6 for the details. This results in the equation

$$-\frac{\sin\beta}{\beta}\left(R + \frac{b^2}{12R}\right)2\beta Rb + 2\left(-R\sin\gamma + \frac{w}{2}\cos\gamma\right)\cdot bw = 0 \tag{9}$$

After inserting $\beta = \frac{\pi}{2} - \frac{\alpha}{2}$ hence $\sin\beta = \cos\gamma$, the solution of $\frac{R}{w}$ can be found:

$$\boxed{\begin{aligned} \frac{R}{w} &= \frac{q}{2}\left[\sqrt{2 - p + \tan^2\left(\frac{\alpha}{2}\right)} - \tan\left(\frac{\alpha}{2}\right)\right] \\ q &= 1 \\ p &= \frac{1}{3}c^2 \end{aligned}} \tag{10}$$

Note that not every combination of c and α is possible. Since $R > r$ must hold, for a given scale parameter c there's a maximum possible joint angle α_{max}. There would also be a minimal possible (negative) angle since the blades shouldn't overlap. Not discussed here for none of the boomerang types. Result:

$$\alpha_{max} = 2\arctan\left(\frac{3 - 2c^2}{3c}\right) \tag{11}$$

For $c > \frac{\sqrt{3}}{\sqrt{2}} \approx 1.22$ no possible boomerang shape exists.
For this rather crude shape the following approximation (simply $c = 0$) can be used for most classical boomerangs in practical use. It has an accuracy of 1% for $c = 0.2$ and 4% for $c = 0.5$

for all possible joint angles α. However note that the influence of the shape of the blade is more important than the influence of c itself.

$$\frac{R}{w} = \frac{1}{2}\left[\sqrt{2+\tan^2\left(\frac{\alpha}{2}\right)} - \tan\left(\frac{\alpha}{2}\right)\right] \tag{12}$$

4.2.2 Omega boomerang

For an omega-shaped boomerang (see Fig. 3) I proceed similarly as above and solve the equation for an annulus sector, two small rectangles and two rectangles:

$$-\left(R+\frac{b^2}{12R}\right)\frac{\sin\gamma}{\beta}2\beta Rb + 2\left(R\cos\gamma + \frac{b}{4}\sin\gamma\right)\frac{b^2}{2} + 2\left(R+\frac{b+w}{2}\right)\cos\gamma\cdot bw = 0 \tag{13}$$

Note that for the omega shape, $\sin\beta = \sin\gamma$. The solution is

$$\boxed{\begin{aligned} \frac{R}{w} &= \frac{1}{2\tan\left(\frac{\alpha}{2}\right)}\left[q+\sqrt{q^2+2p\tan\left(\frac{\alpha}{2}\right)+\frac{1}{6}c^2\tan^2\left(\frac{\alpha}{2}\right)}\right] \\ q &= 1+\frac{c}{2} \\ p &= 1+c \end{aligned}} \tag{14}$$

The formula for the maximum angle is rather complicated. Condition here: The small rectangles must not overlap. See Fig. 3. But a reasonable choice of b and w ($c < 1$) avoids impossible shapes.

$$\begin{aligned} A &= 5c^2 \\ B &= 6\left(c^2-4c-2\right) \\ C &= -12c \end{aligned}$$

$$\alpha_{max} = 2\arctan\left(\frac{-B+\sqrt{B^2-4AC}}{2A}\right)$$

For the maximum scaling parameter ($c = 2$), $\alpha_{max} = 133.3° > 0°$. So no further restrictions for c here.
The following approximation may only be used for very slim shapes: accuracy 1% for $c = 0.02$, accuracy 5% for $c = 0.1$.

$$\frac{R}{w} = \frac{1}{2\tan\left(\frac{\alpha}{2}\right)}\left[1+\sqrt{1+2\tan\left(\frac{\alpha}{2}\right)}\right] \tag{15}$$

Later on surprisingly I found that slightly modified forms of Eqns. 12 and 15 serve as accurate approximations for both two bladed types.

4.3 Boomerangs with semistadium shaped blades

I don't yet provide approximations in this section as the goal is to have exact formulae. The structure of the results remains the same. Just the values for p and q have to be replaced.

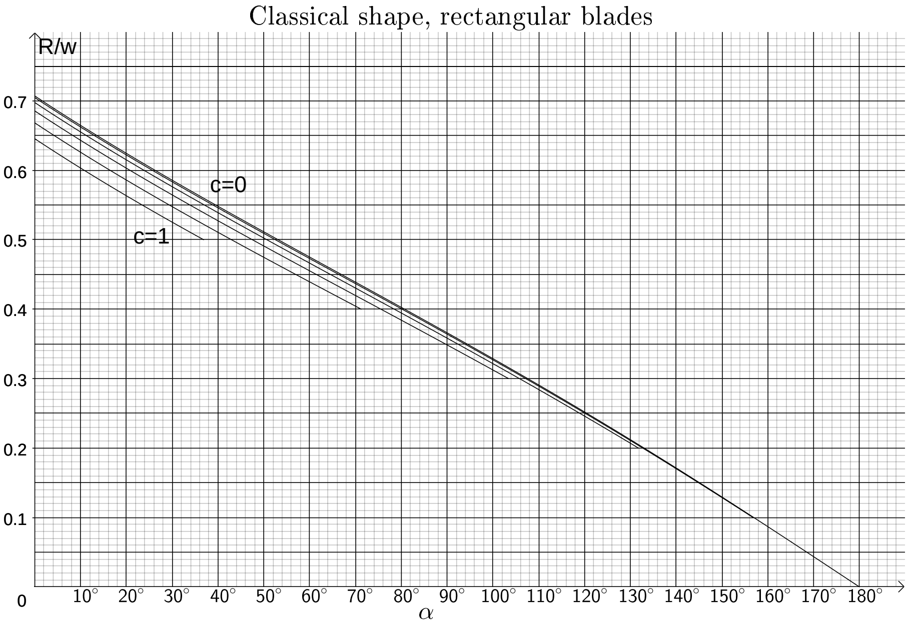

Figure 7: Lookup graphics for classical boomerang with rectangular blades, (Eq. 10) for c from 0 to 1 by steps of 0.2.

4.3.1 Classical boomerang

Putting together the necessary boomerang elements (two additional semicircles compared to Eq. 9) I get the equation

$$\begin{aligned} &-\frac{\sin\beta}{\beta}\left(R+\frac{b^2}{12R}\right)2\beta Rb+2\left[-R\sin\gamma+\left(\frac{w}{2}-\frac{b}{4}\right)\cos\gamma\right]\left(w-\frac{b}{2}\right)b \\ &+2\left[-R\sin\gamma+\left(w-\frac{b}{2}+\frac{2b}{3\pi}\right)\cos\gamma\right]\frac{\pi}{8}b^2=0 \end{aligned} \tag{16}$$

to solve. $\sin\beta=\cos\gamma$. Result:

$$\boxed{\begin{aligned} \frac{R}{w}&=\frac{q}{2}\left[\sqrt{2-p+\tan^2\left(\frac{\alpha}{2}\right)}-\tan\left(\frac{\alpha}{2}\right)\right] \\ q&=\left(1-\frac{1}{2}c+\frac{\pi}{8}c\right) \\ p&=\frac{\pi^2c^2}{32q^2} \end{aligned}} \tag{17}$$

The maximum possible angle is calculated as before. Result:

$$\alpha_{max}=2\arctan\left(\frac{8-2c\,(4-\pi)-c^2\,(2+\pi)}{8c-c^2\,(4-\pi)}\right) \tag{18}$$

If $c=\frac{\pi-4+\sqrt{32+\pi^2}}{\pi+2}\approx 1.09$, Eq. 18 returns $\alpha_{max}=0$. So no shape possible for $c\geq 1.09$.

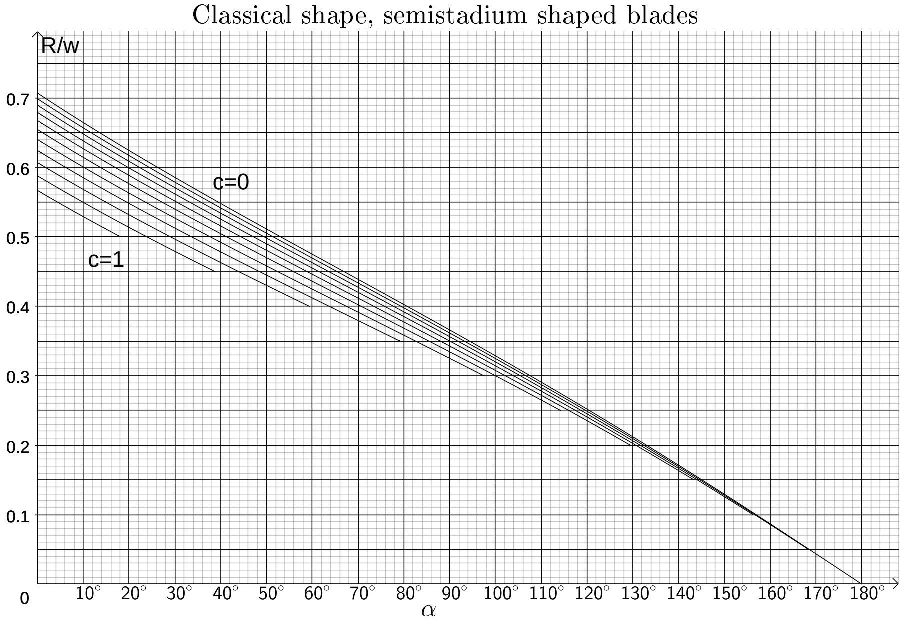

Figure 8: Lookup graphics for classical boomerang with semistadium shaped blades, (Eq. 17) for c from 0 to 1 by steps of 0.1.

4.3.2 Omega boomerang

For this case the equation to solve is

$$\begin{aligned}&-\left(R+\frac{b^2}{12R}\right)\frac{\sin\beta}{\beta}2\beta Rb+2\left(R\cos\gamma+\frac{b}{4}\sin\gamma\right)\frac{b^2}{2}\\&+2\left(R+\frac{w}{2}+\frac{b}{4}\right)\cos\gamma\left(w-\frac{b}{2}\right)b+2\left(R+w+\frac{2b}{3\pi}\right)\cos\gamma\frac{\pi b^2}{8}=0\end{aligned}\tag{19}$$

Compared to Eq. 13 it contains again an additional term for the semicircles. The solution ($\sin\beta = \sin\gamma$) is

$$\boxed{\begin{aligned}&\frac{R}{w}=\frac{1}{2\tan\left(\frac{\alpha}{2}\right)}\left[q+\sqrt{q^2+2p\tan\left(\frac{\alpha}{2}\right)+\frac{1}{6}c^2\tan^2\left(\frac{\alpha}{2}\right)}\right]\\&q=1+\frac{\pi}{8}c\\&p=1+\frac{\pi}{4}c-\frac{1}{12}c^2\end{aligned}}\tag{20}$$

The formula for the maximum angle is rather complicated. Condition here: The small rectangles must not overlap. See Fig. 3. But a reasonable choice of b and w ($c < 1$) avoids impossible shapes.

$$\begin{aligned}A&=10c^2\\B&=c^2(26-3\pi)-6c(4+\pi)-24\\C&=3c^2(4-\pi)-24c\end{aligned}$$

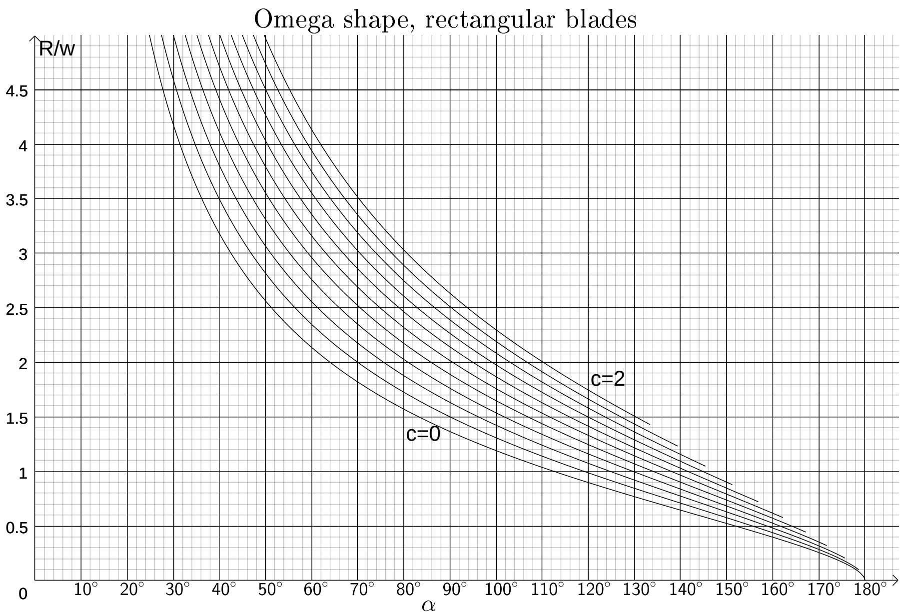

Figure 9: Lookup graphics for omega boomerang with rectangular blades (Eq. 14) for c from 0 to 2 by steps of 0.2.

$$\alpha_{max} = 2 \arctan\left(\frac{-B + \sqrt{B^2 - 4AC}}{2A}\right)$$

For $c = 2$, the maximum scaling parameter, $\alpha_{max} \approx 117° > 0°$. So no further restrictions for c here.

4.4 Approximations for semistadium shaped blades

I found simple ad hoc approximations based on the very basic Eqns.12 and 15 for both cases. Accuracy 0.3% or better for classical shape for all possible values of c:

$$\boxed{\frac{R}{w} = \frac{1 - 0.101c}{2}\left[\sqrt{2 - 0.4c^2 + \tan^2\left(\frac{\alpha}{2}\right)} - \tan\left(\frac{\alpha}{2}\right)\right]} \tag{21}$$

For the omega shape, the accuracy is at least 0.8% for $30° \leq \alpha \leq 120°$ and at least 2% for $10° \leq \alpha \leq 140°$ for all possible values of c.

$$\boxed{\frac{R}{w} = \frac{1 + 0.395c - 0.017c^2}{2\tan\left(\frac{\alpha}{2}\right)}\left[1 + \sqrt{1 + 2\tan\left(\frac{\alpha}{2}\right)}\right]} \tag{22}$$

4.5 How to construct a balanced boomerang.

If you prefer not to use any formulae: The following instructions allow it. Just proportional calculation is needed. Shown for semistadium shaped blades, same procedure with rectangular blades. Just choose the appropriate graphs among Fig. 7, 8, 9 and 10.

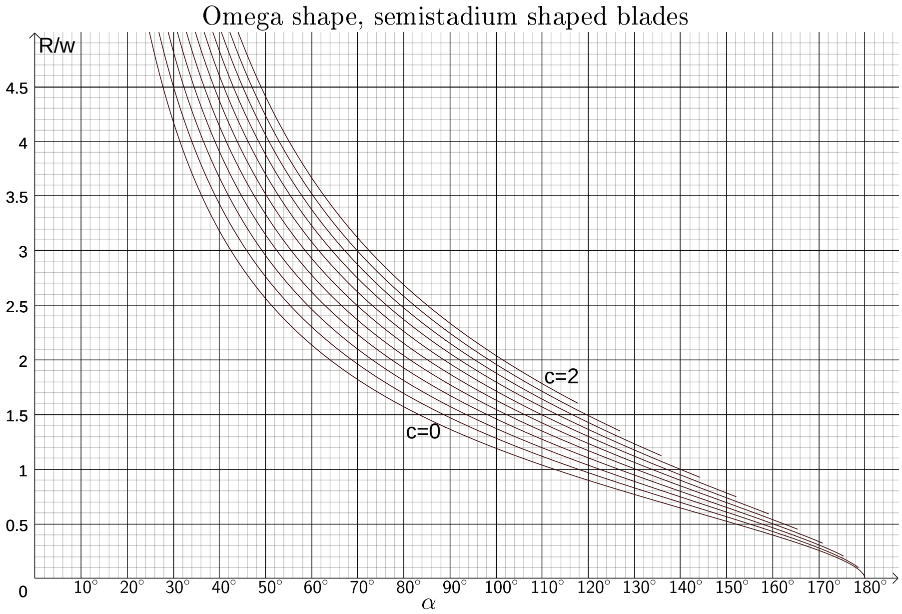

Figure 10: Lookup graphics for omega boomerang with semistadium shaped blades (Eq. 20) for c from 0 to 2 by steps of 0.2.

4.5.1 Classical type, semistadium shaped blades

Decide first, how large the joint angle α, blade length w and -width b shall be. We take $\alpha = 80°$ $w = 22$ cm and $b = 4$ cm as in Fig. 3. Now compute $c = \frac{4}{22} = 0.182$ and check Fig. 8. On the x-axis search for 80, pick the line corresponding to 0.2 (that's the third line from the top) and read the y-value: That's $\frac{R}{\ell} = 0.39 - 0.40$, let's say 0.395. Now multiply with w: $R = 0.395 \times 22 = 8.69$ cm. That corresponds well with the value in Fig. 3.
So you need an annulus sector with angle $180° - 80° = 100°$, inner radius $R - \frac{b}{2} = 6.7$ cm and outer radius $R + \frac{b}{2} = 10.7$ cm, two rectangles of $\ell = w - \frac{b}{2} = 22 - 2 = 20$ cm times $b = 4$ cm and two semicircles with radius $r = \frac{b}{2} = 2$ cm. Even a standard MS Office program like power point can draw these pieces. If your boomerang is too small/too large: Just scale it.

4.5.2 Omega type, semistadium shaped blades

Example again as in Fig. 3: $\alpha = 120°$, $w = 9.5$ cm, $b = 3$ cm. So $c = 0.316$. Look up the y-value in Fig. 10, between second and third lowest line at 120 degrees. That's just slightly more than 1.0 because 0.316 is only very slightly closer to 0.4 than 0.3. Let's say 1.01. Now $R = 1.01 \cdot 9.5 = 9.60$ cm.
So you need an annulus sector with angle $360° - 120° = 240°$, inner radius $R - \frac{b}{2} = 8.1$ cm and outer radius $R + \frac{b}{2} = 11.1$ cm. Two small rectangles of $b = 3$ cm times $\frac{b}{2} = 1.5$ cm, two rectangles of $\ell = w - \frac{b}{2} = 8$ cm times $b = 3$ cm and two semicircles with radius $r = \frac{b}{2} = 1.5$ cm. Even a standard MS Office program like power point can draw these pieces.
What about a "fat" omega with $\alpha = 160°$, $b = 6$ cm, $w = 5$ cm? $c = 1.2$. But the 7th lowest line in Fig. 10 ends at 152°. Not a possible choice.

4.6 General multi bladed boomerangs with balanced c.o.m.

Third possibility: A multi bladed boomerang with central hole/ring of outer radius R and N blades which may vary in length ℓ and width b. The width of the central hold/ring is arbitrary since this part is balanced in any case. The basic idea: If wings 1 to $N-1$ are geometrically defined, wing N can be calculated.

4.6.1 Rectangular blades

The expression $q_i = A_i\vec{r}_i$ for each blade i used for the calculation of the c.o.m. is

$$\boxed{q_i = b_i\ell_i\left(R + \frac{1}{2}\ell_i\right)} \tag{23}$$

I don't express the equations in terms of the blade length as this complicates the expressions a lot. However using complex numbers gives a more compact form of the equation for a c.o.m at the origin:

$$\sum_{i=1}^{N} q_i e^{i\varphi_i} = 0 \text{ or for determining blade } N\text{:}$$

$$\sum_{i=1}^{N-1} q_i e^{i\varphi_i} + q_N e^{i\varphi_N} = 0$$

If blades $1 \ldots N-1$ are specified (q_i as function of b_i, ℓ_i and R), the position angle φ_N of blade N and q_N can be extracted from

$$q_N e^{i\varphi_N} = -\sum_{i=1}^{N-1} q_i e^{i\varphi_i} \tag{24}$$

If calculating with spreadsheets, these definitions (now going back to real numbers) make it much easier:

$$\boxed{\begin{aligned} s_x &= -\sum_{i=1}^{N-1} q_i \cos\varphi_i \\ s_y &= -\sum_{i=1}^{N-1} q_i \sin\varphi_i \end{aligned}} \tag{25}$$

Then it follows directly that blade N has the properties

$$\boxed{\begin{aligned} q_N &= \sqrt{s_x^2 + s_y^2} \text{ and} \\ \varphi_N &= \arctan 2\left(\frac{s_y}{s_x}\right) \end{aligned}} \tag{26}$$

where $\arctan 2$ is the 4 quadrant inverse tangent function. In excel enter $atan2(s_x, s_y)$. To get a relation between ℓ_N and b_N, insert $i = N$ into Eq. 23:

$$q_N = b_N\ell_N\left(R + \frac{1}{2}\ell_N\right) \tag{27}$$

If you choose a certain ℓ_N, the corresponding width is

$$\boxed{b_N = \frac{2q_N}{2R + \ell_N}} \tag{28}$$

Vice versa Eq. 27 has to be solved for ℓ_N. Result:

$$\boxed{\ell_N = -R + \sqrt{R^2 + 2\frac{q_N}{b_N}}} \tag{29}$$

4.6.2 Semistadium shaped blades

If you want a more realistic model (necessary if $c > 0.2$, for extremely asymmetric shapes even for smaller c), this is the choice. The blades are now composed of a rectangle and a semicircle. Equation 23 has to be modified:

$$\boxed{q_i = b_i\ell_i\left(R + \frac{1}{2}\ell_i\right) + \frac{1}{4}b_i^2\left(\frac{\pi}{2}R + \frac{\pi}{2}\ell_i + \frac{1}{3}b_i\right)} \tag{30}$$

Equations 25 to 26 stay the same.
For a given b_N, ℓ_N can be calculated with

$$\boxed{\ell_N = -\left(R + \frac{\pi}{8}b_N\right) + \sqrt{\left(R + \frac{\pi}{8}b_N\right)^2 + 2\frac{q_N}{b_N} - \frac{\pi}{4}Rb_N - \frac{1}{6}b_N^2}} \tag{31}$$

For a given ℓ_N (less common in practical use) a cubic equation in b_N would have to be solved.

5 Discussion of some results

When comparing the results from Eq. 17 shown in Fig. 8 and Eq. 10 shown in Fig. 7 with "Dabbes" calculations in [2], Eq. 10 reproduces Dabbes results very closely. In Table 1 just a difference of magnitude 0.1% can be seen. I can't explain this minor difference, but fur sure it is not because of the semistadium shaped blades. Maybe he considered even the airfoil since he indicated the thickness in his results. Considering the semistadium shaped blades changes the results for w by more than 2% since $c > 0.2$ as displayed in Table 1.
We clearly see that considering the blade shape is of higher importance than just c alone. For a certain c, blades with semistadium shape must be a bit longer than rectangular blades. That makes sense, as removing material from rectangular wings needs compensation. Only possibility is longer wings. Or reversely spoken: For equal blade length w, the boomerang with semistadium shaped blades has a slightly smaller annulus radius R. See Fig. 11. For the omega shape, the difference between the radii is slightly more pronounced.
Interestingly, for two bladed boomerangs, the results for rectangular blades are of minor significance since the approximations for semistadium shaped blades are based on the most simple Eqns.15 and 12.

6 Conclusion

I confirmed "Dabbes" results from 1987 (rectangular blades) except for a systematic deviation of 0.1%. Additionally I provided equations for calculating general multi bladed boomerangs, omega shapes and the classical shape. The equations for semistadium shaped blades are not significantly more complex than those for the rectangular blades. To my surprise, the simplified set of equations for the two bladed boomerangs I found, is based on the most simple equations for $\frac{R}{w}$ for blades of zero width ($c = 0$) rather than "Dabbes" results. I didn't investigate whether a 5% discrepancy in

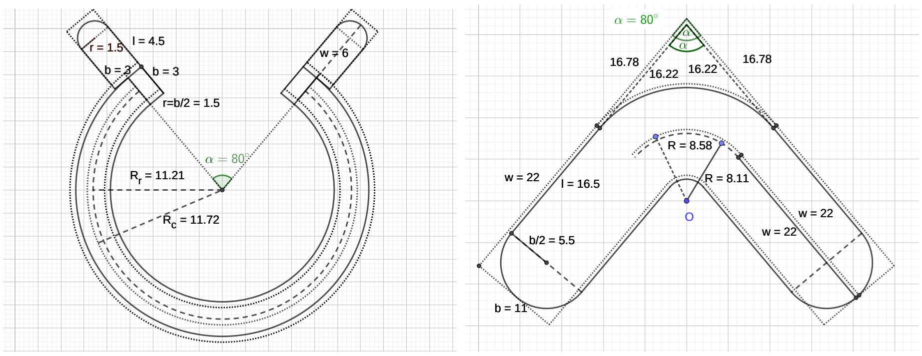

Figure 11: Omega- and classical shape, both blade types for $c = 0.5$. For two boomerang pairs with equal blade length w, the contour of the semistadium shaped version (solid line) has a slightly smaller annulus radius than the rectangular one (dashed line). $R_r < R_c$.

$\alpha[°]$	b	R	$\ell = w$	$\ell_d = w_d$	w_r round	$\frac{w_r}{w_d}$	$c_r = \frac{b}{w_r}$	$c_d = \frac{b}{w_d}$
50	40	70	138.2	138.0	142.3	1.032	0.281	0.290
55	40	70	143.2	143.0	147.4	1.031	0.271	0.279
60	40	70	148.6	148.4	152.8	1.030	0.262	0.269
65	40	70	154.4	154.2	158.6	1.028	0.252	0.259
70	40	70	160.7	160.5	164.9	1.027	0.243	0.249
75	40	70	167.5	167.3	171.7	1.026	0.233	0.239
80	40	70	175.0	174.8	179.2	1.025	0.223	0.229
85	40	70	183.2	183.0	187.4	1.024	0.213	0.218
90	40	70	192.3	192.1	196.5	1.023	0.204	0.208
95	40	70	202.5	202.2	206.7	1.022	0.194	0.198
100	40	70	213.9	213.6	218.1	1.021	0.183	0.187
105	40	70	226.8	226.5	231.0	1.020	0.173	0.176
110	40	70	241.6	241.3	245.8	1.019	0.163	0.166
115	40	70	258.7	258.3	262.9	1.018	0.152	0.155
120	40	70	278.6	278.3	282.8	1.016	0.141	0.144

Table 1: All lengths in mm. Comparison of Eq. 10 and 17 (semistadium shaped blades with subscript w_r) with "Dabbes" results (w_d) from 1987 for a constant R. The discrepancy of 0.1% between w_d and w cannot be explained. Maybe the airfoil which slightly concentrates the mass towards the center of the wings? We clearly see, that considering the blade shape is of higher importance than the latter. Semistadium shapeb blades must be a few % longer than rectangular blades.

the calculated radius can be spotted by eye during the flight of the boomerang or not. There's no evidence that these kind of boomerangs perform "better", but they might be helpful to calculate the flightpath of boomerangs as the aerodynamic properties of a centred annulus sector might match the properties of a complete ring quite closely.

References

[1] E. Mawick V. Behrens W. Bretfeld. “nr. 1/87”. In: *Bumerangwelt* (1987).

[2] E. Mawick V. Behrens W. Bretfeld. “II/87”. In: *Bumerangwelt* (1987).

[3] Prasad Gudem, Manuel Schütz, and Kyle Holland. “Flight Dynamics of Boomerangs: Impact of Reversal of Airflow, Reversal of Angle-of-Attack and Asymmetric Lift”. In: *AIAA Aviation 2019 Forum*. DOI: 10.2514/6.2019-2826. eprint: https://arc.aiaa.org/doi/pdf/10.2514/6.2019-2826. URL: https://arc.aiaa.org/doi/abs/10.2514/6.2019-2826.

[4] F. Hess. *Boomerangs, Aerodynamics and Motion*. Rijksuniversiteit te Groningen, 1975. URL: https://books.google.ch/books?id=OPNOAAAAMAAJ.

[5] John Vassberg. “Boomerang Flight Dynamics”. In: *30th AIAA Applied Aerodynamics Conference*. DOI: 10.2514/6.2012-2650. eprint: https://arc.aiaa.org/doi/pdf/10.2514/6.2012-2650. URL: https://arc.aiaa.org/doi/abs/10.2514/6.2012-2650.

[6] A. Adler. In: (1985). URL: http://aerobie.narod.ru/aerobie.htm.

[7] R. Flay, A. Piard, and P. Bot. “Aerodynamics of a highly cambered circular arc aerofoil : experimental investigations”. In: 2017.

[8] M. Siems. *Die neue Bumerangmappe*. Im Selbstverlag, Hirschberg/Grosssachsen, Germany, 1995. ISBN: 3980169510.

[9] E. Mawick V. Behrens W. Bretfeld. “II/95”. In: *Bumerangwelt* (1995).